Mediterranean Geoscience Reviews (2024) 6:249–268
https://doi.org/10.1007/s42990-024-00138-2

ORIGINAL PAPER

Impact of spatial resolution on soil loss estimation: a case study of abandoned quarries in Morocco

Nabil Aouichaty[1] · **Yahya Koulali**[1]

Received: 6 May 2024 / Revised: 11 August 2024 / Accepted: 13 August 2024 / Published online: 2 September 2024

Abstract
Soil erosion poses significant challenges to sustainable land management. The Revised Universal Soil Loss Equation (RUSLE) has emerged as a valuable tool for predicting soil-erosion risk, providing essential insights for effective soil-conservation practices. However, the accuracy of RUSLE predictions strongly depends on the quality and suitability of the input data. This study investigated the impact of variability in the input data on the performance of the RUSLE model in quantifying soil-erosion rates for abandoned quarries in the Bouguergouh commune in Morocco using two sets of input data. The first set represents coarse resolution data (30 m) extracted from different available sources (ISRIC for soil data, NASA database for weather data, Landsat 8 for land use, and ASTER Digital Elevation Model (DEM) for elevation data). These data were compared with a high-resolution (10 m) dataset comprising field data for soil, observed weather data from the Bouregreg and Chaouia Hydraulic Basin Agency data extracted from the Mohammed VI satellites at 0.5 m, and a DEM from Sentinel-1A at 10 m. Our findings reveal that the erosion rates obtained from both the measured (10 m) and international (10 m) databases, using the LS (10 m) factor set, exhibit significant and comparable values. Specifically, the erosion rates ranged from 1.28 to 7.7 t/ha/yr for the measured database and from 1.25 to 7.74 t/ha/yr for the international database. Based on the results of this study, international databases can estimate soil losses using high-resolution DEMs instead of investing in time-consuming soil sampling and analysis results or acquiring expensive high-resolution satellite images, however, conducting the same comparison in other areas can generate global conclusions.

Keywords Abandoned quarries · Soil loss · RUSLE · GIS · DEM · Databases

1 Introduction

Water erosion manifests as the degradation of surface soil layers, accompanied by the displacement of constituent materials (Antoni et al. 2006), driven by the energy generated from raindrop impact and the subsequent transport of soil particles from their original positions (Kinnell 2016). This is one of the leading causes of soil degradation worldwide (Ranieri et al. 2002), posing a significant threat to human society and the environment (Singh et al. 2007). The affected land area is estimated to be 1100 million hectares worldwide (Saha 2003), underscoring its severity globally, especially in vulnerable regions. Mediterranean nations face heightened risks with their challenging topography, irregular rainfall patterns, high temperatures, and soil erodibility. This holds true for Morocco, where similar issues threaten soil health (Bleu and Antipolis 2003).

Soil erosion monitoring is often limited in various parts of the world, making global modeling applications crucial for comprehending the extent of soil erosion and its environmental impact. Furthermore, soil-erosion modeling is a practical and reliable tool for assessing erosion and selecting appropriate erosion management strategies (Dargiri and Samsampour 2023). Various models with differing input requirements and complexities have been developed recently (Dargiri and Samsampour 2023; Keller et al. 2021). Widely used models include the Universal Soil Loss Equation (USLE) (Borrelli et al. 2021; Dargiri and Samsampour 2023; Wischmeier and Smith 1978), the Revised Universal Soil Loss Equation (RUSLE) (Dargiri and Samsampour 2023; Thapa 2020), the Soil and Water Assessment Tool

✉ Nabil Aouichaty
aouichaty.nabil@gmail.com

[1] Hassan First University of Settat, Faculty of Sciences and Techniques, Moroccan Agro-Resources and Environment (ARME) Team, Settat, Morocco

(SWAT) (Arnold et al. 2012), and the Water Erosion Prediction Project (WEPP) (Dargiri and Samsampour 2023).

These models aim to estimate soil loss and formulate-conservation measures (Zhang et al. 2016), with the choice of model depending on the availability and adaptability of the data to the study area (Dargiri and Samsampour 2023; Salumbo 2020). Currently, the USLE and RUSLE models, known for their simplicity, ease of use, and data availability, are widely used for assessing global soil erosion. However, these methods have limitations, such as the inability to account for gully erosion in calculations and restrictions in assessing soil losses at all locations or for every wet event (Brahim et al. 2020).

Recently, GIS and remote sensing have been integrated into soil-erosion calculations, allowing for spatial representation of soil loss over large areas and developing scenarios for human interventions (Bonn 1998; Bou Kheir et al. 2006; Chafai et al. 2020; Shrimali et al. 2001). GIS facilitates the integration of maps, databases, and mathematical equations, providing a cost-effective, time-efficient, and accurate measurement of soil erosion and its geographic spread over extensive territories (Millward and Mersey 1999; Wang et al. 2003).

Many studies (Aouichaty et al. 2024; Bagwan and Gavali 2024; Hoffmann et al. 2013) conclude that RUSLE model users should prioritize using high-resolution input data to capture topography's effects on soil erosion accurately. The lower-resolution data can significantly underestimate the erosion risk. Despite the importance of spatial resolution, the search results indicate a lack of research specifically focused on this issue for RUSLE modeling in abandoned quarry environments. Most studies have examined the impact of resolution in larger watershed or regional scales, but more work is needed to understand the nuances of these unique quarry sites (Aouichaty et al. 2024). The search also reveals other challenges related to soil erosion in abandoned quarries in Morocco (Aouichaty et al. 2022), such as:

- Abandoned quarries often become uncontrolled waste sites, further contributing to pollution and health risks in surrounding areas.
- The natural regeneration of vegetation in abandoned quarries is slow, leaving the exposed soil vulnerable to erosion.
- Quarrying activities, in general, put pressure on already limited soil and water resources in the semi-arid Moroccan environment, accelerating erosion processes.

This study presents a case analysis of five abandoned quarries (Aouichaty et al. 2021, 2022) using the RUSLE model and GIS to assess and create a map of water erosion in the semiarid region of Morocco. The RUSLE model, with parameters (rainfall erosivity, soil erodibility, topographic factor, vegetation cover factor, and anti-erosion practices factor) established in previous Moroccan studies (Bou-imajjane et al. 2020; El Jazouli et al. 2019; Modeste et al. 2016; Tahiri et al. 2015), was chosen due to data availability in the commune of Bouguergouh. The model was applied to identify and quantify soil losses resulting from sheet and gully erosion, spatializing them by creating erosion risk maps. In addition, this study focused on evaluating the impact of data quality on erosion rates of RUSLE results.

One of the aims of this study was to determine the optimum resolution that would guarantee the best performance and represent reality. To this end, the international database with a 30 m resolution and the measured database with a 10 m resolution for the Bouguergouh commune were compared to select the most significant model between these two resolutions. At the end of this study, another comparison was made between the two databases (international and measured), revealing the optimum resolution for the communities (Fig. 1).

2 Materials and methods

2.1 Study area

The study area is in Bouguergouh (a rural commune in Settat Province), at a latitude of 33° 11′ 72.94″ N and a longitude of 7° 33′ 30.68″ W. It extends over approximately 102 km^2 with altitudes between 360 and 635 m (Fig. 2). The climate is semiarid, with an average annual temperature of approximately 17.4 °C (minimum 10.5 °C and maximum 32.5 °C). The average rainfall is approximately 394 mm/year (2000–2017), with irregular rainfall (Aouichaty et al. 2022). According to Bouslihim et al. (2019), June, July, and August are typically the driest months, whereas December, January, and February are the wettest months (Fig. 3a). Over the 18 years (2000–2017), there was a notable fluctuation in the yearly average precipitation data, with several extended dry spells (2001, 2015, and 2017) interspersed with shorter cycles of wetter weather (Fig. 3b). In addition, this area contains clay deposits, which are prone to developing badlands. Numerous clay quarries are also present, some of which are abandoned (Aouichaty et al. 2022).

2.2 Presentation of the RUSEL model and methodology

The Revised Universal Soil Loss Equation (RUSLE) is the revised version of the USLE method (Renard et al. 1996). The RUSLE model permits evaluating the average annual soil-loss rate and the geographical distribution of soil erosion. It is the most commonly employed model for

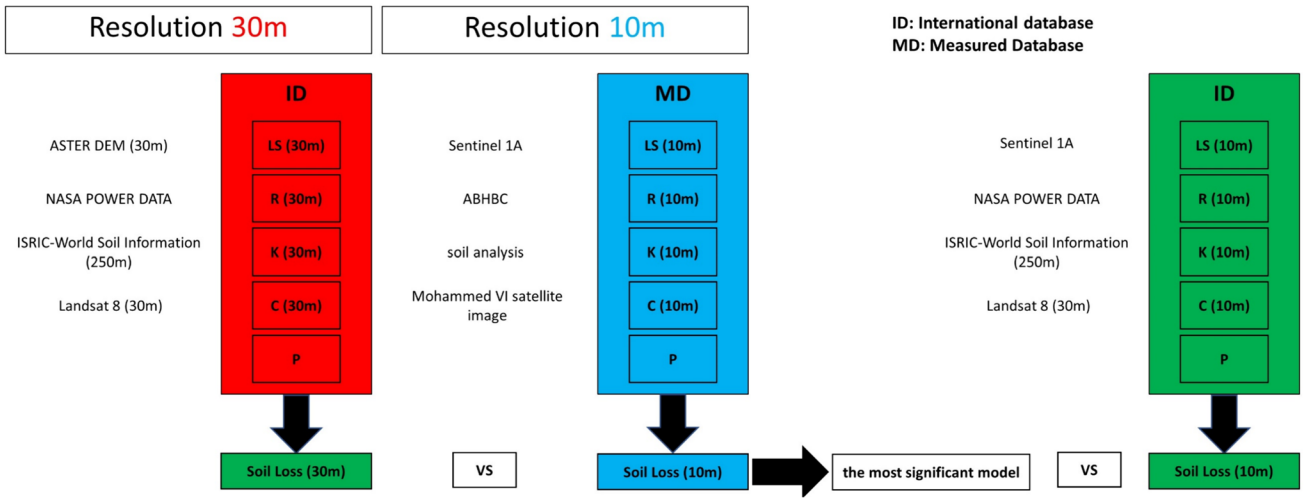

Fig. 1 Descriptive diagram of the methodology adopted

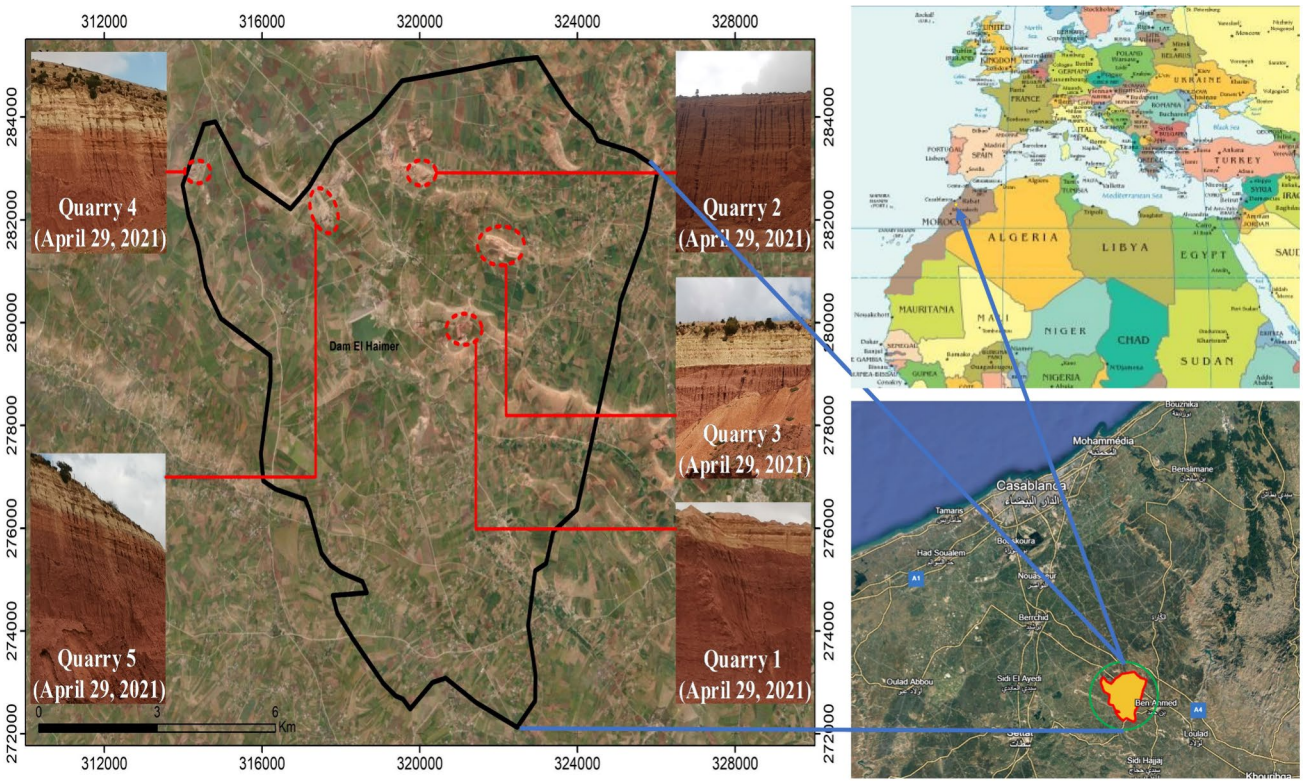

Fig. 2 Geographic distribution of abandoned quarries

determining soil loss and devising soil-conservation strategies to mitigate water erosion (El Jazouli et al. 2019).

Diverse inputs (factors) that mimic reality, with different resolutions and scales based on the study objectives, are necessary to assess and map erosion accurately. These inputs represent factors that influence erosion, such as topography (LS), land use (*C*), climate (R), and soil conditions (*K*). The methodology adopted to analyze the effects of these factors and how their resolution may lead to different RUSLE results is presented in Fig. 1.

Soil loss (*A*) was estimated via the RUSLE equation based on a multiplicative function that considers five factors: rainfall erosivity (*R*), soil erodibility (*K*), topographic factor (LS), vegetation cover factor (*C*), and anti-erosion

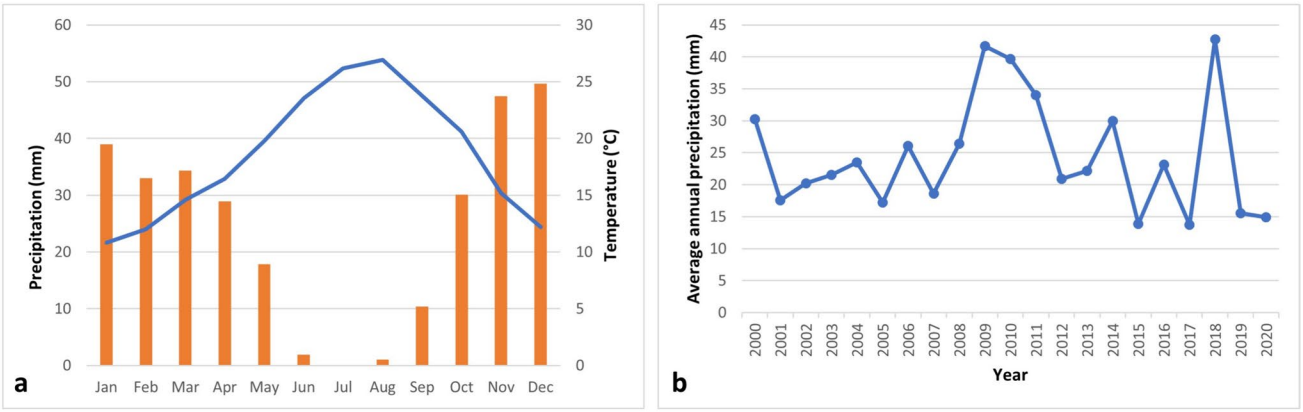

Fig. 3 **a** Variations in the monthly average rainfall and temperature, and **b** mean annual precipitation between 2000 and 2020 in Bouguergouh

practices factor (*P*). Accounting for these five factors is crucial for accurately assessing soil loss and devising effective erosion control strategies (Aouichaty et al. 2022; Karamesouti et al. 2016). These different factors were analyzed in ArcGIS software (version 10.5) (Abdi et al. 2023; Aouichaty et al. 2022; Bagwan and Gavali 2024; Hagos et al. 2023; Renard et al. 1996; Weslati and Serbaji 2024).

$$A = R.\ K.\ LS.\ C.P \tag{1}$$

The erosivity of rainfall (*R*-factor) depends mainly on climatic data, as precipitation significantly generates erosion risks and patterns (Brahim et al. 2020; Ghosal and Bhattacharya 2020). In this work, we used two rainfall databases covering more than 20 years. The first database was downloaded from the National Aeronautics and Space Administration (NASA) Power Data Access Viewer database for 14 stations distributed throughout the Settat Province. The second database was obtained from the Bouregreg and Chaouia Hydraulic Basin Agency (ABHBC) for the four weather stations (Tamedroust, Oulad M'hamed, Sidi Ahmed Ben Ali, and El Mers) (Fig. 4).

To produce the erosivity map, the *R*-factor was calculated (Eq. 2) (Rango and Arnoldus 1987) for each station. The Kriging model has been used in several works, and good results have been obtained (Allafta and Opp 2021; El Jazouli et al. 2017; Kashiwar et al. 2022). Therefore, this method was chosen to interpolate the R values.

$$\log R = 1.74 * \log \sum \left(\frac{p_i^2}{p} \right) + 1.29 \tag{2}$$

where R is the rainfall erosivity index (MJ mm/ha h yr), P_i is the average monthly precipitation (mm), and P is the average annual precipitation (mm).

The second factor is soil erodibility (*K*-factor), which indicates the degree of vulnerability of soil to erosion. It is determined based on soil parameters, including soil texture (sands, clays, and silts) and organic carbon. In the present study, two databases were used. The necessary parameters were extracted

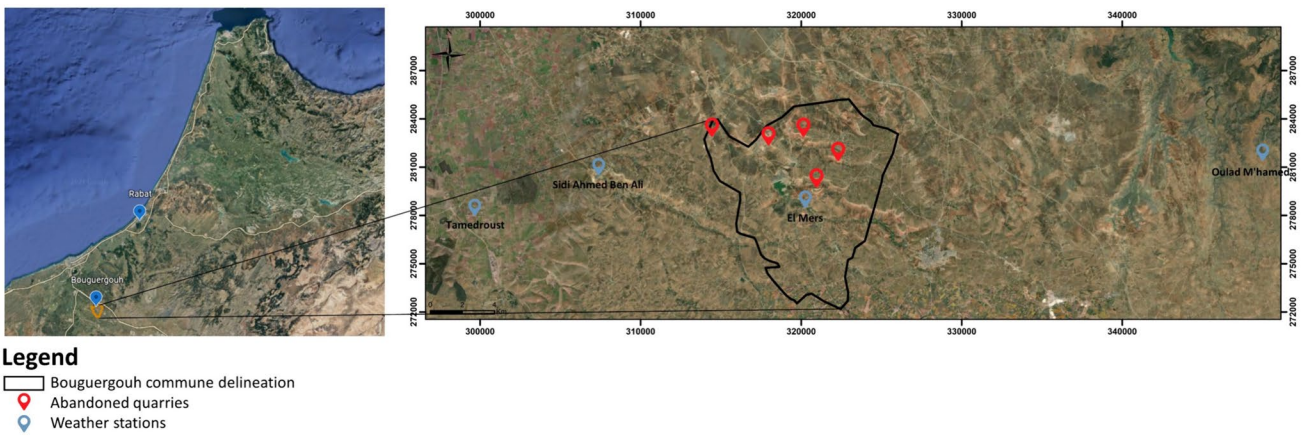

Fig. 4 Location of abandoned quarries relative to weather stations

first from the International Soil Reference and Information Centre (ISRIC)—World Soil Information database in raster form with a resolution of 250 m. For the second soil database, 28 samples (0–20 cm depth) were collected across the study area to characterize the different soil types (Fig. 5).

The soil erodibility map of the study area was produced in ArcGIS software (version 10.5), and the following equation was used (Neitsch et al. 2000; Williams and Singh 1995).

$$K_{\text{usle}} = f_{\text{csand}} \times f_{\text{cl-si}} \times f_{\text{orgc}} \times f_{\text{hisand}} \times 0.1317, \quad (3)$$

where K_{usle} is the soil erodibility index (t ha h/ha MJ mm) (Erdogan et al. 2007); f_{csand} is a factor that lowers the K indicator in soils with high coarse sand content and increases it for soils with low sand content; $f_{\text{cl-si}}$ gives low erodibility factors for soils with high clay/silt ratio; and f_{orgc} reduces K values in soils with high organic-carbon content, while f_{hisand} lowers the K values for soils with very high sand content. The factors are calculated:

$$f_{\text{csand}} = 0.2 + 0.3 \times e^{-0.256 \times m_s \left(1 - \frac{m_{\text{silt}}}{100}\right)}, \quad (4)$$

$$f_{\text{cl-si}} = \left(\frac{m_{\text{silt}}}{m_C + m_{\text{silt}}}\right)^{0.3}, \quad (5)$$

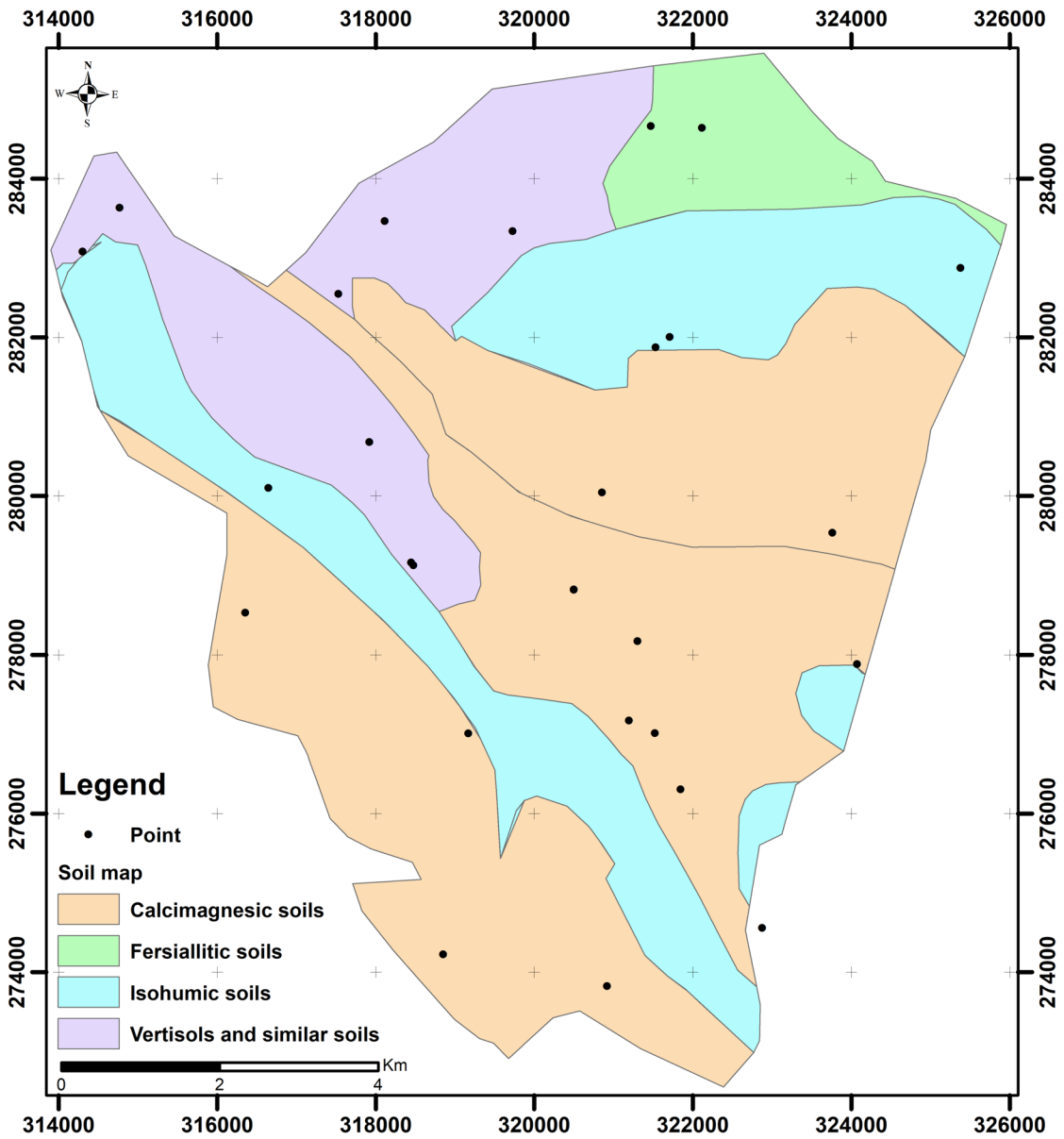

Fig. 5 The Bouguergouh soil map (soil map of central Morocco)

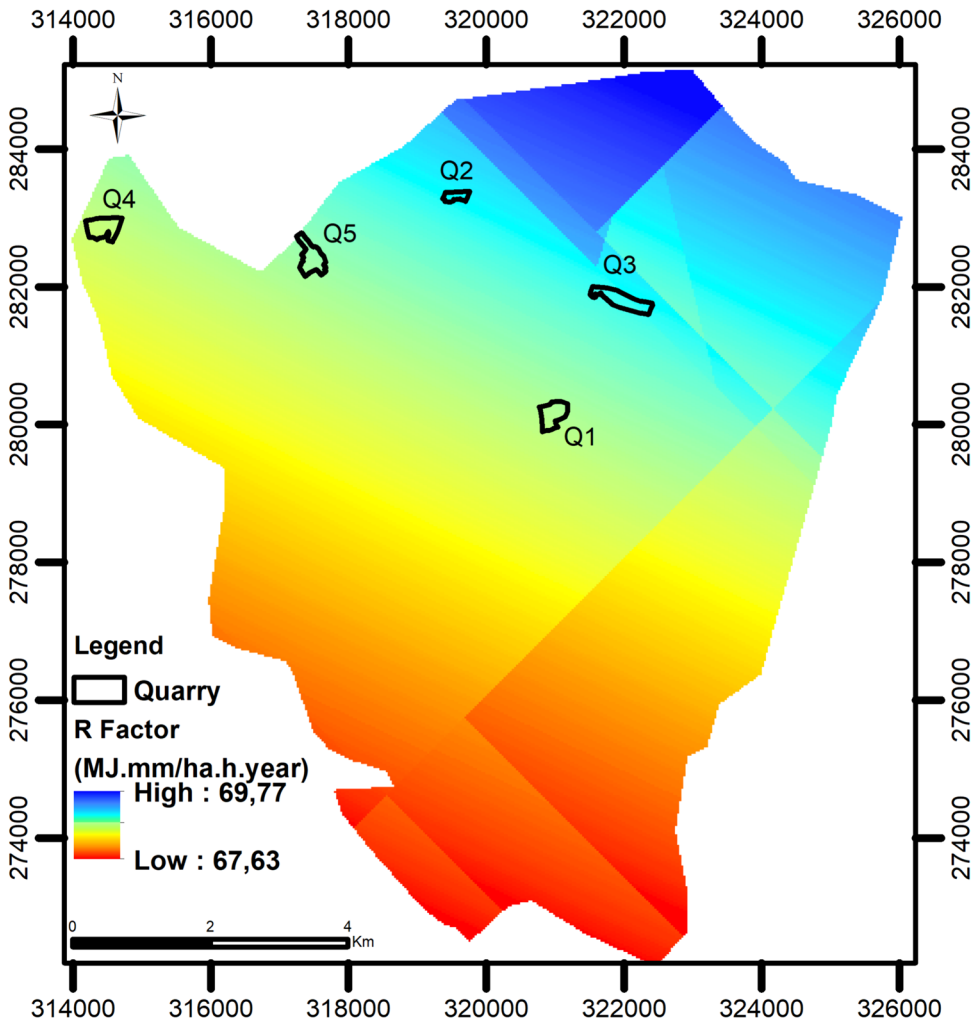

Fig. 6 *R*-factor map for NASA Power Data

$$f_{\text{orgc}} = 1 - \frac{0.25 \times \text{org}C}{\text{org}C + e^{3.72-2.95\times\text{org}C}}, \tag{6}$$

$$f_{\text{hisand}} = 1 - \frac{0.7 \times \left(1 - \frac{m_s}{100}\right)}{\left(\frac{1-m_s}{100}\right) + e^{-5.51+22.9\times\left(1-\frac{m_s}{100}\right)}}, \tag{7}$$

where m_s is the percentage of sand (0.05–2.00 mm diameter), m_{silt} is the percentage of silt (0.002–0.05 mm diameter), m_C is the percentage of clay (< 0.002 mm diameter), and org*C* is the percentage of organic carbon in the layer (%) (Devatha et al. 2015; Koirala et al. 2019; Kolli et al. 2021).

Next, the LS factor is a parameter that considers a slope's length and steepness. The slope length refers to the distance from the top of the area to where the water starts concentrating in a stream or river. Steep slopes with fast-moving water tend to experience significant erosion (Devatha et al. 2015; El Jazouli et al. 2017; Mitasova et al. 1996). Two DEMs were used to create the LS map: the ASTER DEM (30 m) and the Sentinel-1A DEM (10 m resolution). The LS map was produced by combining data from these two sources.

The spatial analysis toolbox of ArcGIS software was used to generate slope gradient (degree) raster layers, and the flow direction and accumulation matrices were calculated using the hydrology toolbox. The LS factor was calculated based on Eq. 8, developed Hoffmann et al. (2013) and Mitasova et al. (1996) using a raster calculator in ArcGIS software (version 10.5) (Aouichaty et al. 2022; Kamamia et al. 2021).

$$\begin{aligned}\text{LS} = {} & \text{power (flow accumulation} \divideontimes \text{cell resolution)/} \\ & 22.1, 0.4) \divideontimes \text{power ((sin (slope of degree)} \divideontimes 0.01745)/ \\ & 0.09, 1.4) \divideontimes 1.4.\end{aligned} \tag{8}$$

The *C* factor represents the vegetation cover. In the present study, we extracted *C*-factors from two satellite images. Landsat 8 and Mohammed VI satellite images. Landsat 8 images were downloaded from the US Geological Survey (USGS) database with a resolution of 30′ m in July 2021. The second image was extracted from the Mohammed VI

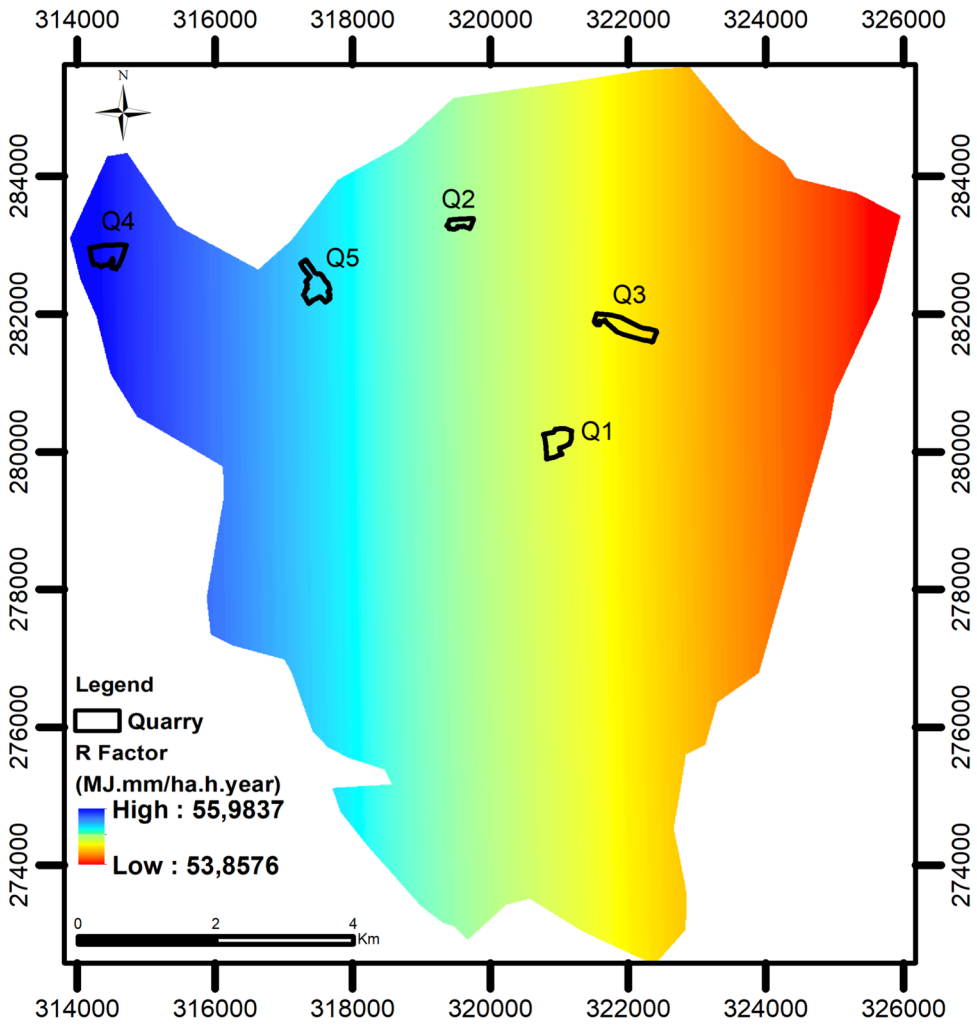

Fig. 7 *R*-factor map for ABHBC

Table 1 *R*-factors for each quarry

Quarry	*R*-factor (NASA power data) (MJ mm/ ha h year)	*R*-factor (ABHBC) (MJ mm/ha h year)
Q1: Bouguergouh	68.69	54.73
Q2: Bouguergouh	69.03	54.97
Q3: Bouguergouh	68.98	54.54
Q4: Bouguergouh	68.63	55.92
Q5: Bouguergouh	68.77	55.35

satellite (A and B). It included 50 cm and four bands (RGB and NIR) under favorable climatic conditions on different dates (July 06, 19, and 31, 2021). The satellite was probably chosen because of its high-quality imaging capabilities, which make them suitable for this type of analysis. As the first Moroccan satellite dedicated to earth observation, Mohammed VI images provide a valuable new data source for researchers wishing to apply advanced remote sensing techniques (El-Harti et al. 2020).

A land-use map across the study area was created by supervised classification of both images (Landsat 8 and Mohammed VI A and B). The *C* factor was converted to a specific value for each class (water body: 0, built-up land: 0.003, forest: 0.004, agriculture: 0.4, uncultivated land: 0.75, bare land: 1) (El Jazouli et al. 2019).

Finally, soil-conservation practices are crucial in mitigating erosion processes; thus, the extent of soil loss may vary depending on the practices implemented. Some examples of erosion control practices include contour cropping, bench reforestation, and ridging (Roose 1996). The *P* factor represents the relationship between soil loss resulting from a specific support practice and the corresponding loss from an upstream or downstream crop (Renard et al. 1996); in our study area, there was no available information regarding the distribution of soil and water conservation practices within the area, so a value of 1 was assigned to the entire region as the *P* factor (Brahim et al. 2020; El Jazouli et al. 2019; Taoufik et al. 2020).

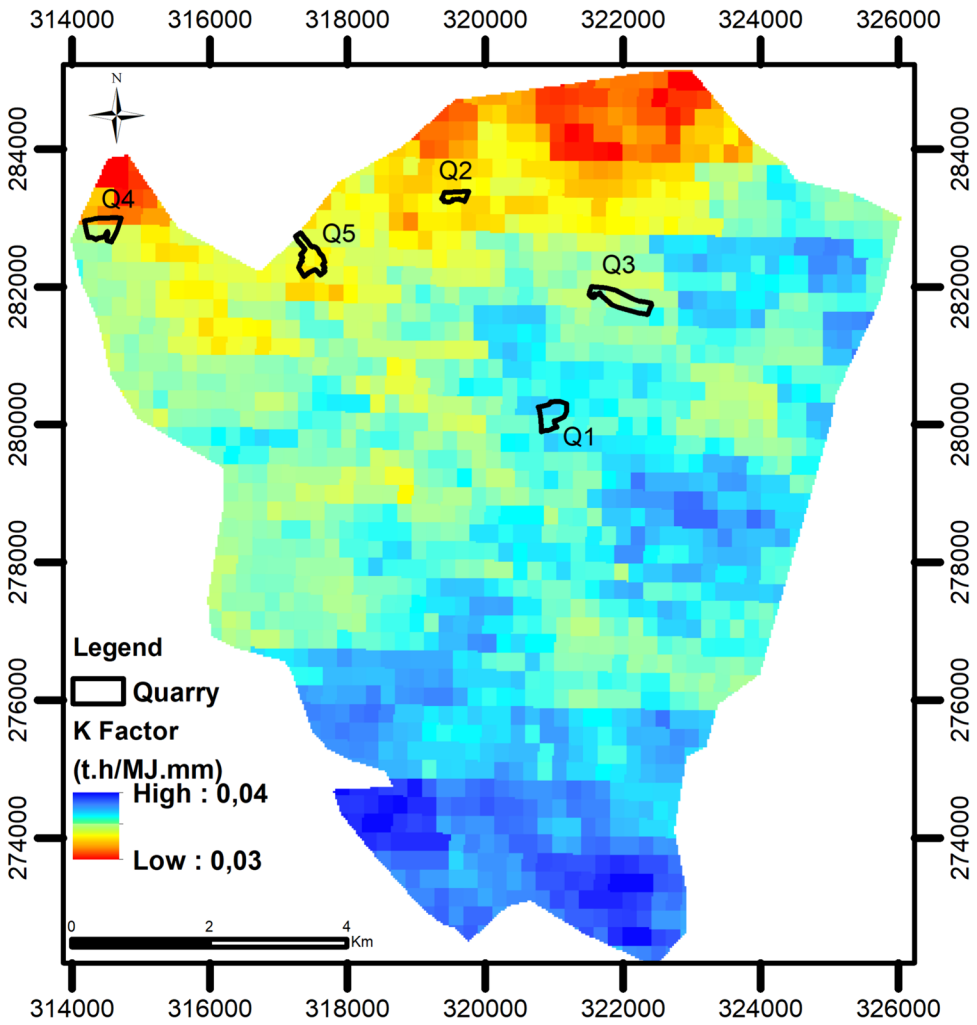

Fig. 8 *K*-factor map for the ISRIC data

3 Results

3.1 Assessment of water *erosion* factors

3.1.1 The R-factor

The precipitation erosivity values were interpolated with ArcGIS version 10.5 software using the geostatistical analysis tool cokriging. The results obtained for the NASA Power Data and the ABHBC data are shown in Figs. 6 and 7, respectively.

Figure 6 shows values ranging from 67.63 MJ mm/ha h year in the southern region to 69.77 MJ mm/ ha h year in the northeastern region of the municipality. Based on the ABHBC data, high erosivity (55.983 MJ mm/ ha h year) is observed in the western region of the municipality and decreases toward the east to 53.857 MJ mm/ ha h year (Fig. 7).

The two data sources summarize the *R*-factor results for the abandoned quarries in the municipality in Table 1.

Quarries experience high erosivity of precipitation: values exceeding 67.69 MJ mm/ha h year according to NASA power data and exceeding 54.54 MJ mm/ha h year according to ABHBC data.

3.1.2 The K-factor

The soil erodibility values were determined with ArcGIS software version 10.5. The results obtained for the ISRIC data and the field sample analysis data are shown in Figs. 8 and 9, respectively.

Generally, the municipality's soil *K*-factor is ≤ 0.05 t h/MJ m indicating very low erodible soil (Dumas 1965).

3.1.3 The LS-factor

The length and slope factors significantly influence soil-erosion processes. The LS factor, calculated using Eq. (8), ranges from 0 to 95.99 for the ASTER DEM at 30 m (Fig. 10) and between 0 and 102,649 for the DEM at 10 m (Fig. 11). Only erosion can affect areas with steep slopes.

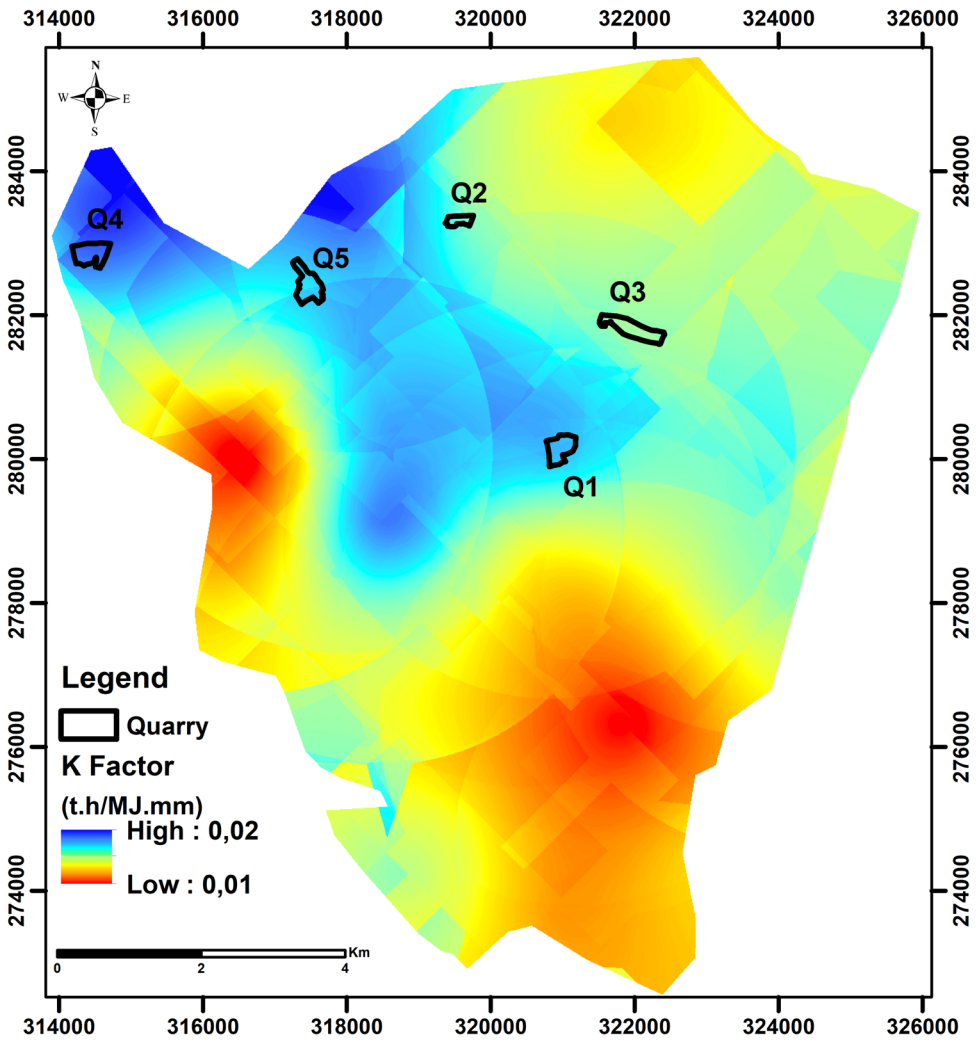

Fig. 9 *K*-factor map for the measured data

The variation in LS results between the two DEMs is related to the difference in resolution.

3.1.4 The C-factor

The annual soil loss from agricultural land varies depending on the crop grown. A greater extent of vegetation cover tends to reduce soil erosion (Maury et al. 2019). The municipality is characterized mainly by bare land (44.48% and 8.12% of the Landsat 8 and Mohamed VI satellite images, respectively) and agricultural and noncultivated land (39.09% and 88.53% of the Landsat 8 and Mohamed VI satellite images, respectively) (Table 2; Figs. 12, 13). Abandoned quarries are considered bare soil.

3.2 Evaluation of soil loss

The municipality's soil loss was evaluated by overlaying the five factors evaluated with ArcGIS tools (version 10.5).

Based on the global database and for a resolution of 30 m, the soil loss varies between 0 and 260.61 t/ha/yr (Fig. 14). For the measured data considered (the ABHBC data, Mohamed VI satellite image, Sentinel-1A image for the DEM 10m and field data), the soil loss varies between 0 and 74.985 t/ha/yr at a resolution of 10 m (Fig. 15).

According to the classification proposed by Beskow et al. (2009) (Table 3), the analysis of soil-loss maps (30 m and 10 m) revealed that the territories of the commune of Bouguergouh were not affected by the same intensity. Indeed, as shown in Table 4:

- The lands with low erosion rates (0–5 t/ha/yr) represent approximately 81% of the total area according to the global databases and 89.57% of the total area according to the measured databases.
- The lands with a high rate (> 15 t/ha/yr) represent 5.75% and 0.98% of the global and measured databases, respectively.

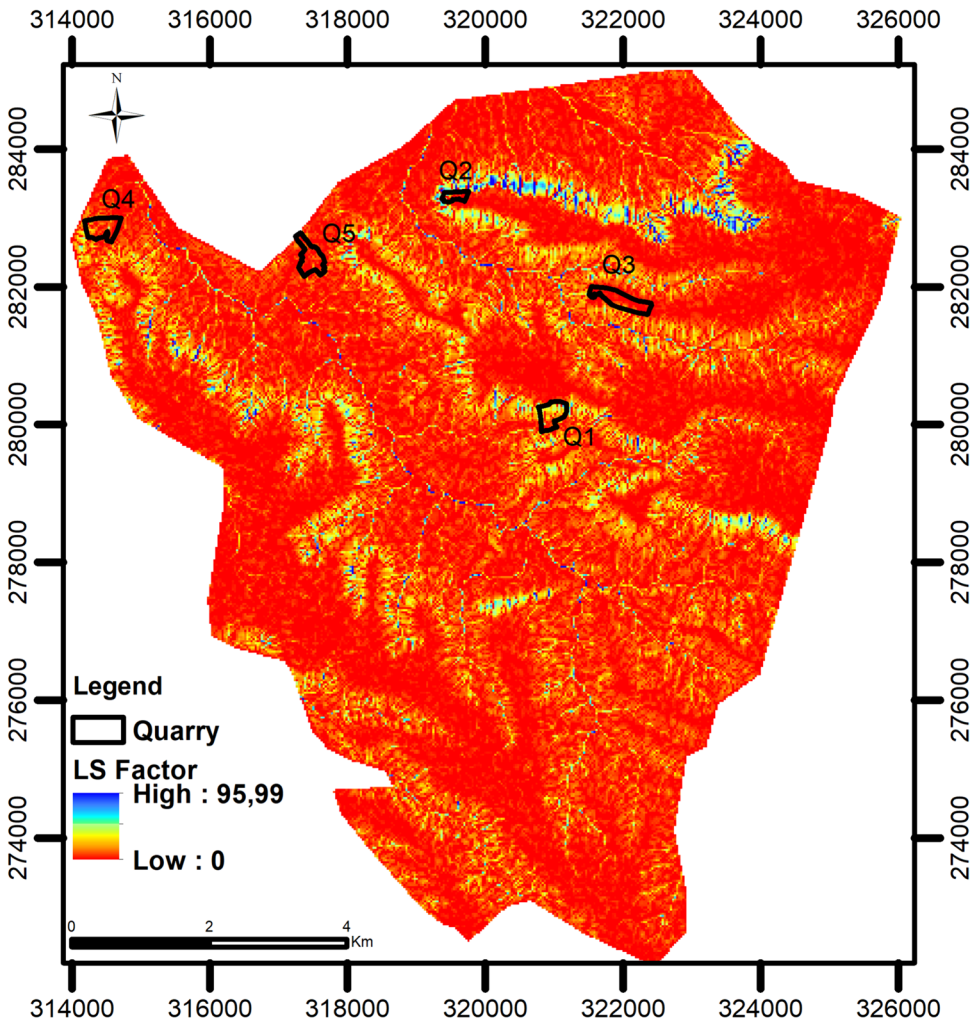

Fig. 10 LS factor map for the DEM (30 m)

This difference is due to the LS factor given the resolution of the DEM (ASTER DEM 30 m and Sentinel 1A [DEM 10 m]), the *R* factor, which is overestimated in the NASA database compared to that of the ABHBC, and the *C* factor, which is more accurate via the Mohamed VI satellite image than via the Landsat 8 image (Table 5).

The results obtained for the sites of the six abandoned quarries (Table 5) showed that quarries Q3, Q4 and Q5 were located in areas where the risk of erosion was low (with a rate varying between 0 and 5 t/ha/yr) and that quarries Q1 and Q2 were located in areas of medium risk (with a rate varying between 5 and 15 t/ha/yr); these results were also obtained for both databases.

High erosion rates can be attributed to a high precipitation rate, represented by the *R* factor, and the topographic conditions characterized by steep slopes (LS factor). This was also confirmed by the presence of several badlands (Fig. 16).

3.3 Influence of the LS factor on the final result

The analysis of the five factors used for the estimation of soil loss reveals that the LS factor (slope related to topography) plays a significant role in the reliability of the results:

- The *K* and *P* values are very similar in the municipality
- The *C* factor is considered bare earth for all quarry sites
- For the *R* factor, the data for international databases such as the ABHBC are deduced from fixed weather stations.

Using the LS factor with the 10 m DEM and the factors *R*, *K*, *C*, and *P* from international databases (with 30 m data resampled to 10 m), raster datasets are converted by tools that follow the resampling method environment interpolate pixel values. In particular, resampling uses the nearest neighbor method to ensure that pixel values are correctly interpolated. The soil loss in the commune of Bouguergouh

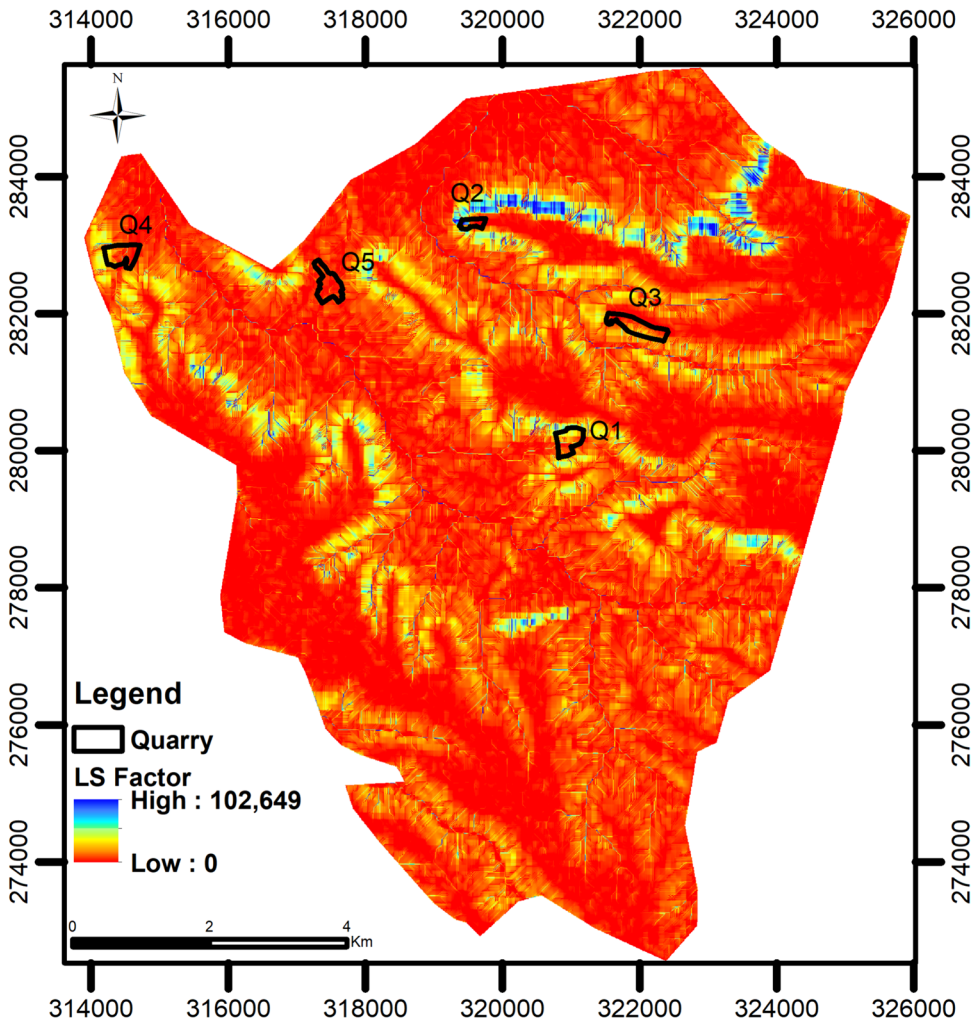

Fig. 11 LS factor map for the DEM (10 m)

varies between 0 and 71.99 t/ha/yr (Fig. 17). This result is comparable to that estimated from the measured data (0–74.98 t/ha/yr) (Table 6).

The estimated soil-loss rate for the five abandoned quarries is given in Table 7. No difference is observed between the measured (Fig. 15) and international (Fig. 17) data.

Table 2 Distribution of vegetation cover in the commune of Bouguergouh

Vegetation cover	Landsat 8		Med VI image	
	Vegetated area (km^2)	Percentage	Vegetated area (km^2)	Percentage
Forest	10.33	11.1	2.48	2.67
Agriculture	23.31	25.04	0.73	0.79
Built-up land	4.64	4.99	0.50	0.54
Bare land	41.41	44.48	7.55	8.12
Uncultivated land	13.08	14.05	81.49	87.53
Water body	0.31	0.34	0.33	0.35

4 Discussion

Our analysis, following the classification proposed by Beskow et al. (2009) (Table 3), revealed variations in erosion intensity in the Bouguergouh commune at resolutions of 30 m (ranging from 0 to 260.61 t/ha/yr) (Fig. 14) and 10 m (0–74.98 t/ha/yr) (Fig. 15). According to global databases, approximately 81% of the land experiences low erosion (0–5 t/ha/yr), while approximately 13.35% faces medium erosion (5–15 t/ha/yr), with 5.75% of the land exhibiting high erosion rates (above 15 t/ha/yr). In contrast, based on the measured databases, 89.57% of the land underwent low erosion, approximately 13.35% experienced medium erosion, and only 0.98% experienced high erosion.

Based on the RUSLE model, the average soil-loss rates for the settlement areas of the five abandoned quarries in the municipality were estimated to be between 1.28 and 7.70 t/ha/yr for the global database and between 0.90 and 7.74 t/ha/yr for the measured database (Table 7).

Taoufik et al. (2020) reported higher values for various abandoned quarries in the Akreuch area, ranging from 9.65

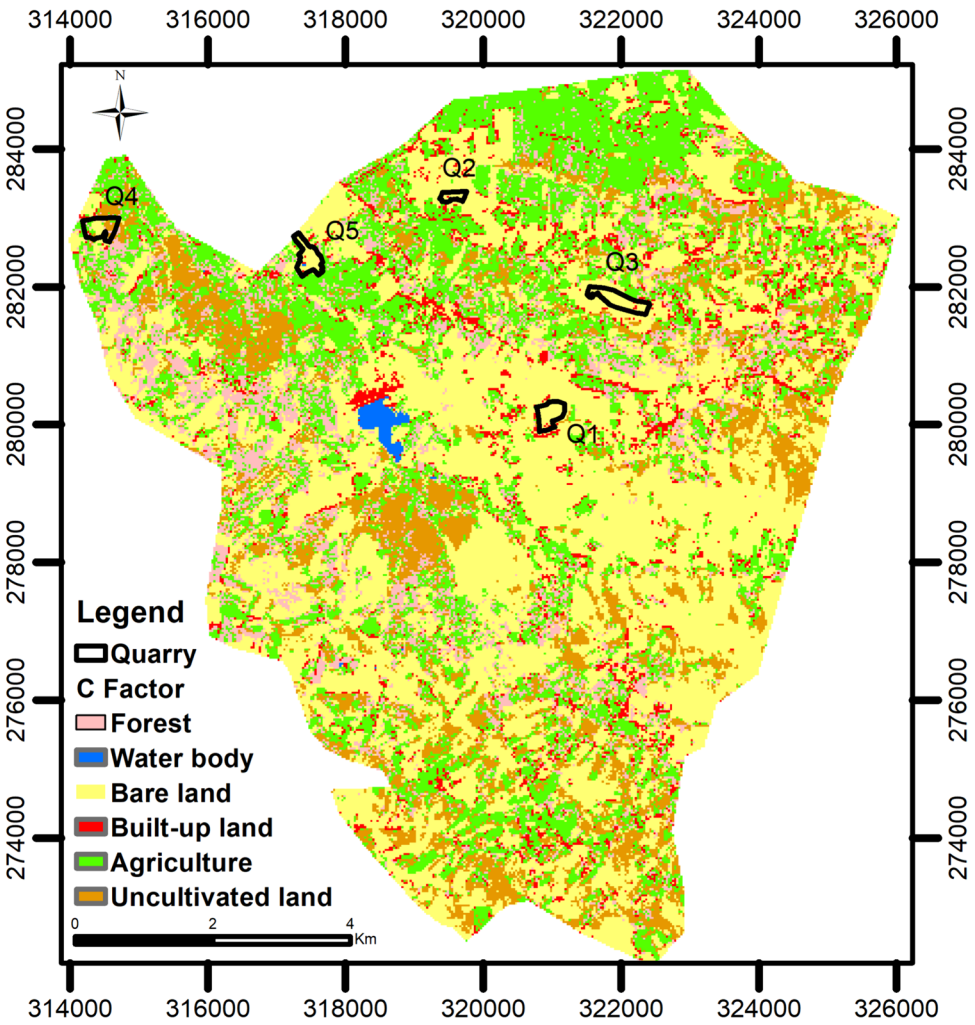

Fig. 12 Factor *C* map for Landsat 8

to 103.46 t/ha/yr. This disparity can be attributed to several factors, including the notably elevated precipitation erosivity factor (*R* factor) exceeding 84 MJ mm/ ha h year. In comparison, our study reports *R*-factors below 68.98 MJ mm/ha h year using the NASA Power Data data and below 55.92 MJ mm/ha h year using the ABHBC database. In addition, there is considerably greater soil erodibility (exceeding 0.07 t h/ MJ mm), whereas our study indicates a lower *K*-factor value. Furthermore, steep slopes characterize the topographic conditions, as indicated by the LS factor.

Integrating data from measured and international databases could enhance soil-loss estimation. We analyzed the five factors within the RUSLE model to assess the data quality.

The *K*-factor values for the commune (ranging from 0.03 to 0.04 t h/MJ mm) appear relatively low compared to findings from other studies on watersheds or abandoned quarries. For instance, Modeste et al. (2016) higher values in the Ourika watershed (High Atlas, Morocco) were reported, ranging from 0.15 to 0.69 t h/ MJ mm. Similarly, Taoufik et al. (2020) identified values exceeding 0.3 t h/ MJ mm in abandoned quarries within the Akreuch region (Morocco). According to the Dumas classification, the soil erodibility factor does not significantly influence this case's erosion rate.

In the case of the *P* factor, we assigned a uniform value of 1 across the entire study area. This decision was made due to insufficient information regarding soil-conservation practices. This approach aligns with previous research studies conducted by Brahim et al. (2020), El Jazouli et al. (2019) and Taoufik et al. (2020), where a similar value was employed under comparable circumstances.

The *C* factor was not a significant influencer in the RUSLE model in our study. This is because the areas where quarries are situated are classified as bare land. This observation supports Taoufik et al. (2020) findings in abandoned quarries in the Akreuch region of Morocco, further confirming our results.

When utilizing NASA Power Data, we observed a range of *R*-factor values for the commune, spanning from 68.63 to 69.03 MJ mm/ha h year. In contrast, our analysis of

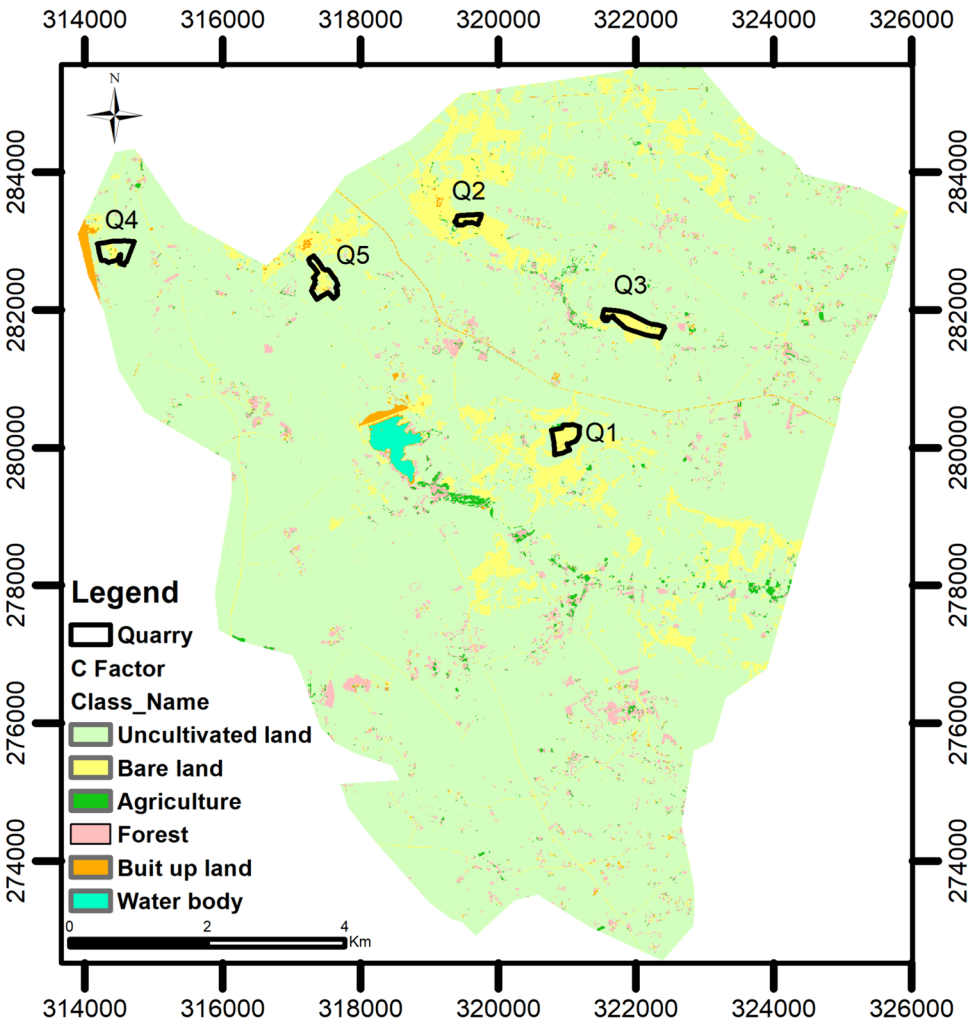

Fig. 13 Factor *C* map for Med-VI images

measured data from the four ABHBC stations located near the Bouguergouh commune, which is within the watershed of Oued El Himer, yielded lower *R*-factors, falling within the range of 53.85–55.98 MJ mm /ha h year. This variance can be attributed to two actors:

- Gaps found in the ABHBC database
- NASA Power Data are estimated at the macro and regional levels.

Other watersheds in similar semiarid climates, as indicated by rainfall data from various Water Basin Agencies, have also been studied. Bou-Imajjane and Belfoul (2020) reported values ranging from 39.18 to 44.56 MJ mm/ha h year in the Beni Mohand watershed in the Western High Atlas of Morocco. Moreover, Bou-Imajjane and Belfoul (2020) reported values between 24.47 and 53.89 MJ mm/ ha h year in the Argana corridor in the High Atlas of Morocco. These two studies yielded values that are generally lower than the results obtained in our research. Similarly, Sadiki et al. (2004) conducted a study in the Boussoaub watershed in the eastern part of the Rif region of Morocco, obtaining values ranging from 31.2 to 60 MJ mm/ ha h year, which aligns with our findings.

In contrast, Taoufik et al. (2020) reported significantly higher values, exceeding 80 MJ mm/ha h year, in the Akreuch region of Morocco. It is worth noting that the precipitation erosivity factor, calculated based on annual rainfall averages, plays a pivotal role in influencing the water erosion rate estimated by the RUSLE model.

The LS factor, which represents topographic characteristics such as slope steepness and length, was a crucial element in our analysis. Previous studies have explored the significance of DEM resolution. For instance, Mondal et al. (2016) utilizing open-source DEMs, including those from the USGS, such as ASTER (30 m), SRTM (30 and 90 m), and GTOPO30 (1 km), as well as data from the National Remote Sensing Center of India (NRSC) for CARTOSAT (30 m). Their findings indicated that high-resolution DEMs at 30 m provided better soil-erosion predictions with reduced

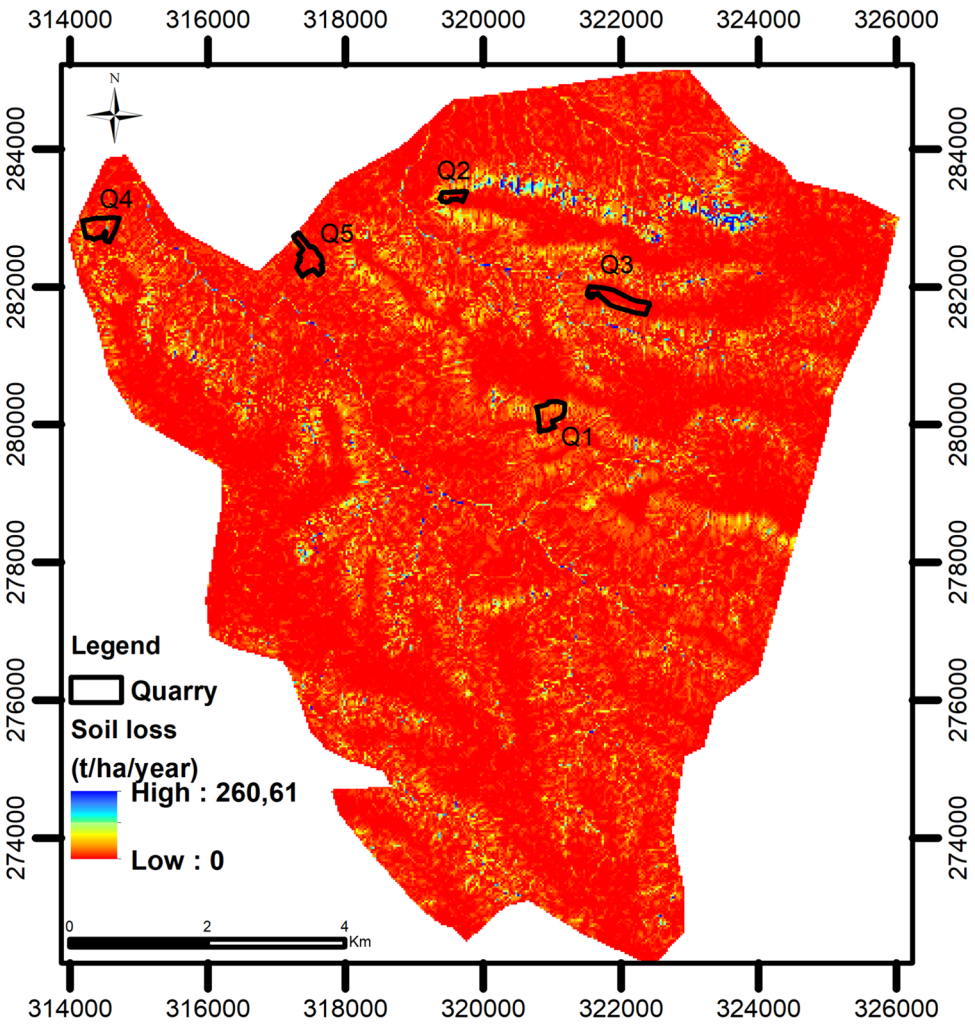

Fig. 14 Soil loss map at t/ha/year for the DEM (30 m)

uncertainty and disparity. Moreover, when they compared different elevation datasets using actual elevation points, they discovered that the 30-m DEM, specifically the SRTM DEM, exhibited superior overall accuracy compared to other DEMs. Similarly, the 30-m DEM yielded more accurate estimates of sediment than the 90 m DEM (Bhattarai and Dutta 2006).

In another comparative study conducted by Shan et al. (2019) in a burned national park in New South Wales, Australia, various DEM resolutions (1, 5, 10, 25, 30, and 90 m) were evaluated. Their research revealed that DEMs in the 5–10 m range provided an optimal resolution that closely aligned with the actual LS values, as measured on 12 plots within the study area. DEMs with resolutions less than 5 m tended to underestimate the LS factor, while those with resolutions greater than 10 m tended to overestimate it.

In the RUSLE model:

- *K*-factor values are shallow (0 and 0.05 t h/MJ mm) in the whole municipality according to both databases (ISRIC-World Soil Information and laboratory data).
- All quarry sites are considered bare land, so the *C* factor is assigned a value of 1.
- The *P* factor is constant and equal to 1 for all of Morocco.
- Only the LS and *R* factors can influence the erosion estimate in the Bouguergouh commune.

Our analysis revealed that the *R* factor, which accounts for precipitation erosivity, was derived from data collected at the four fixed meteorological stations near the commune. Consequently, among the factors in the RUSLE model, the LS factor can be specified and adjusted to fit local conditions.

This study underscores an essential finding: by relying on fundamental international data, we can generate estimates of soil loss that closely approximate actual values. This approach offers several advantages, notably significant cost savings and reduced resource allocation regarding finances and logistics. It prevents the need for extensive soil sampling and analysis and the acquisition of high-cost, high-quality data, satellite imagery, and climate data.

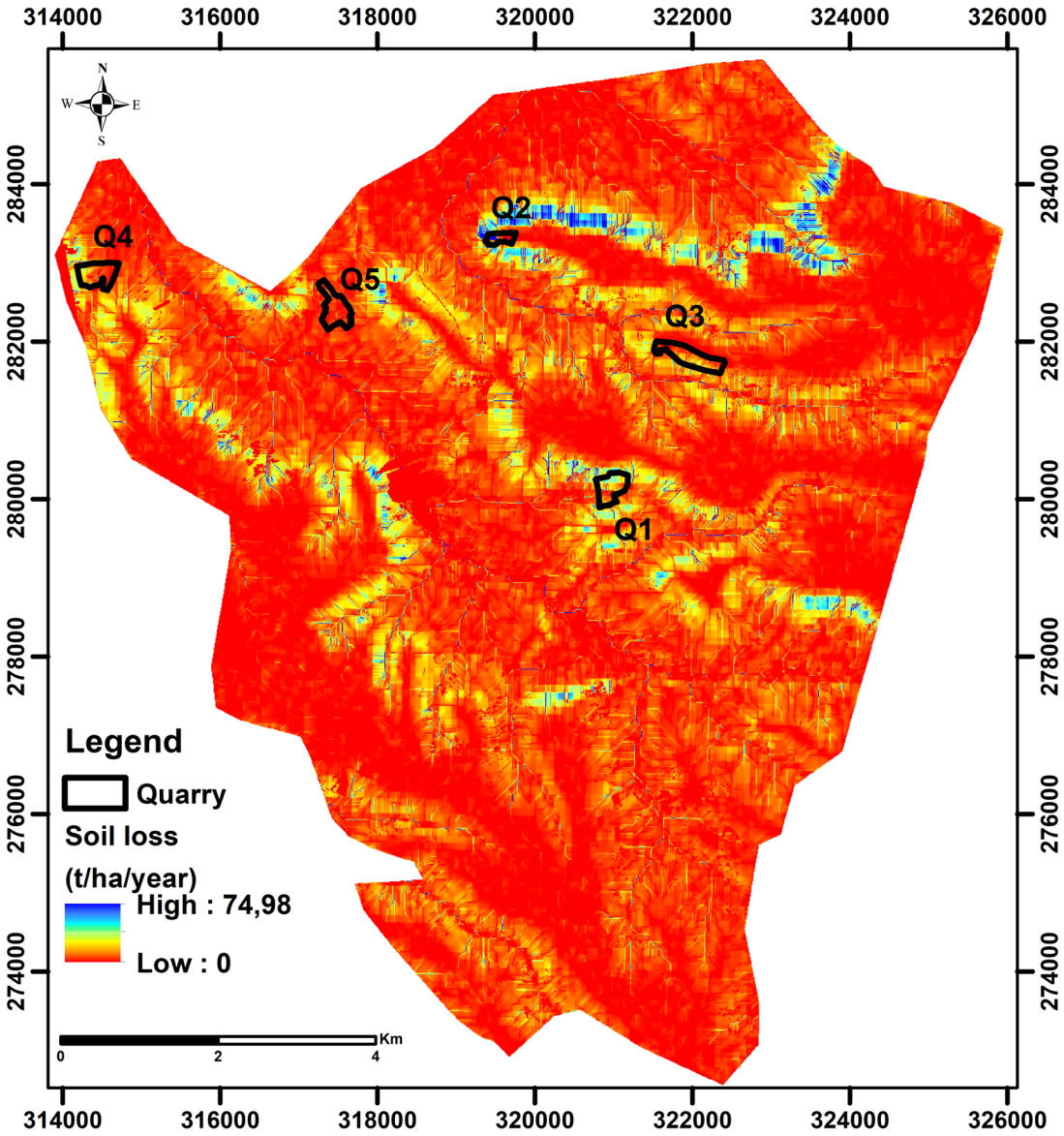

Fig. 15 Resulting soil-loss map at t/ha/year for the DEM (10 m)

Table 3 Soil-loss classes for the province of Settat, adapted from Beskow et al. (2009)

Soil-loss rate (t/ha/yr)	Qualitative soil-loss class
0–5	Low
5–15	Medium
15–25	High
25–100	Very high
> 100	Too high

However, for those seeking even more precise estimations of soil loss, one noteworthy investment to consider is acquiring a high-resolution Digital Elevation Model (DEM). Such an

Table 4 Distribution of the soil-loss rate in the commune of Bouguergouh in the two databases

Soil-loss classification (t/ha/yr)	International databases (30 m)		Measured databases (10 m)	
	Area (km^2)	Percentage	Area (km^2)	Percentage
0–5	75,32	80,90	83,40	89,57
5–15	12,42	13,35	8,80	9,45
15–25	3,04	3,27	0,72	0,77
25–100	2,22	2,39	0,18	0,21
> 100	0,08	0,09		

Table 5 The soil-loss rate for each abandoned quarry

Quarries	Soil-loss rate (30 m) (t/ha/yr)	Soil-loss rate (10 m) (t/ha/yr)
Q1: Bouguergouh	7.74	6.33
Q2: Bouguergouh	6.68	7.7
Q3: Bouguergouh	0.90	2.83
Q4: Bouguergouh	4.83	4.16
Q5: Bouguergouh	1.25	1.28

investment can yield more reliable results and further enhance the accuracy of soil-erosion predictions.

Finally, to combat soil erosion and promote soil conservation, effective solutions include planting cover crops and establishing grassed waterways to protect soil, employing erosion control structures like terracing and check dams to manage runoff, and adopting soil-management practices such as reduced tillage and incorporating organic matter. Implementing water-management strategies like rainwater harvesting and proper drainage, creating riparian buffers to stabilize water bodies, providing education and training to farmers, advocating for supportive policies and financial incentives, and conducting regular monitoring and research are all crucial. These measures collectively enhance soil health and reduce erosion, supporting sustainable land management.

5 Acknowledgment of limitations and recommendations

This study acknowledges its limitations, such as variability in data resolution, inherent limitations of the RUSLE model, and the use of uniform parameters (e.g., P coefficients) due to a lack of local data. Further case studies in different geographical areas and longitudinal studies over a long period are recommended to improve the reliability of the results. Integrating advanced technologies such as high-resolution satellite imagery and LiDAR, as well as considering socioeconomic factors and comparative analyses with other soil-erosion models, can further validate and refine the conclusions.

We recommend the following strategies and considerations for improving soil-erosion estimation and management, particularly in the context of abandoned quarries:

- A high-resolution DEM (1 m or 5 m) was used to improve the results obtained for erosion estimation at a 30 m resolution. Indeed, at the scale of a quarry, the 30-m DEM is

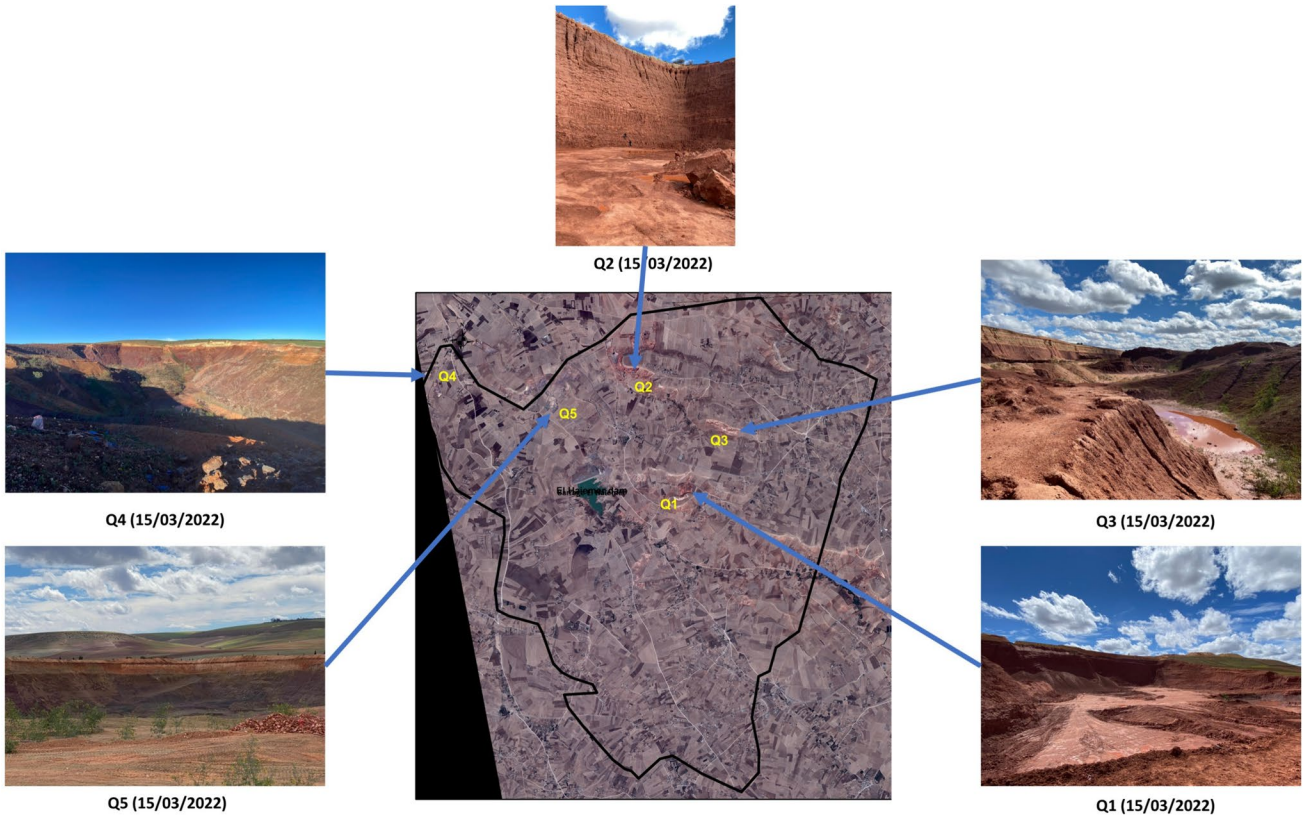

Fig. 16 Images of various eroded open-pit quarries

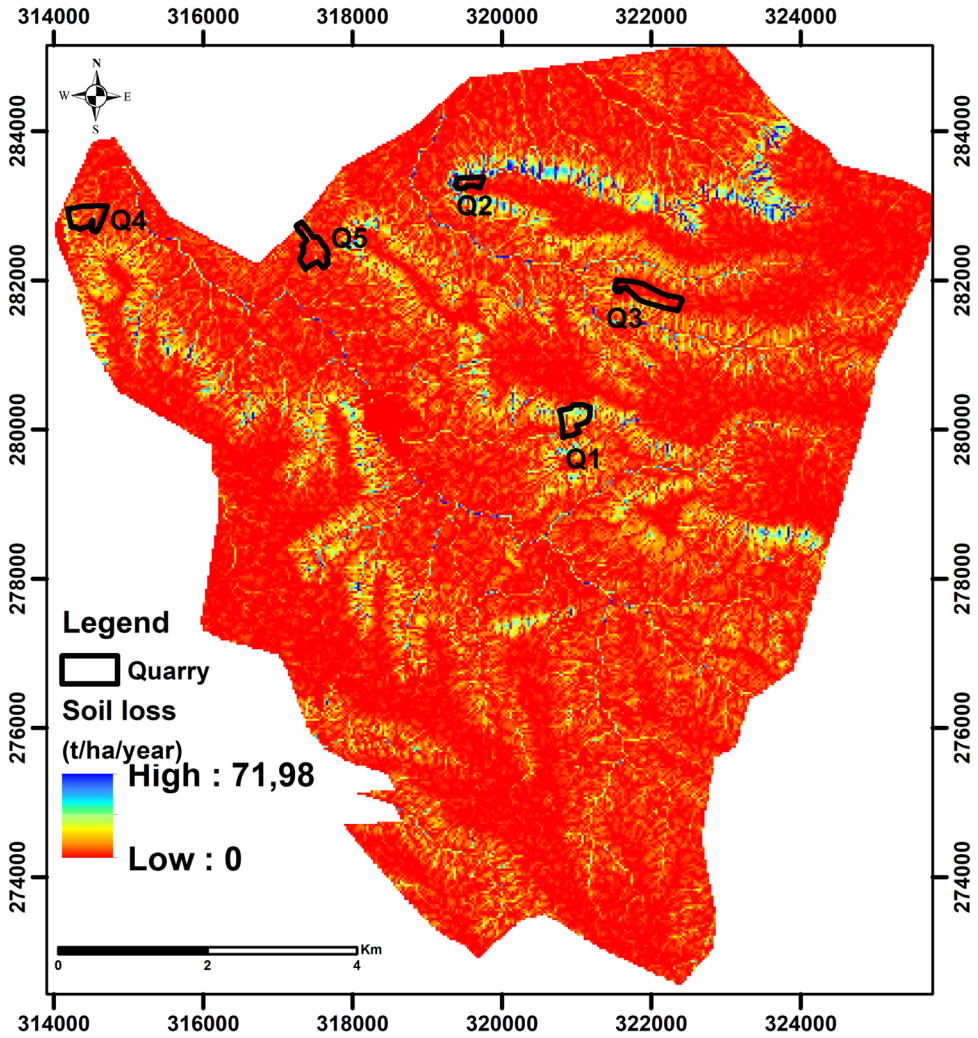

Fig. 17 Soil loss in the commune of Bouguergouh using the 10 m DEM with international data

not very significant because it does not reflect the natural topography of the land

- Drones can be used for topographic surveys because this modern and innovative method allows accurate and detailed land surveys to be conducted faster, more precisely, and more economically than traditional methods
- The quality of precipitation data collected from weather stations should be ensured to avoid gaps in the ABHBC database

Table 6 Distribution of the soil-loss rate in the commune of Bouguergouh according to the two databases at a 10 m resolution

Soil-loss classification (t/ha/yr)	International databases (30 m)		Measured databases (10 m)	
	Area (km^2)	Percentage	Area (km^2)	Percentage
0–5	83,33	89,50	83,40	89,57
5–15	8,40	9,02	8,80	9,45
15–25	1,07	1,14	0,72	0,77
25–100	0,31	0,34	0,18	0,21

6 Conclusion

During this work, the RUSLE factors obtained from international data (NASA, ISRIC, Landsat 8, ASTER DEM 30 m and DEM 10 m obtained from Sentinel 1A converted by SNAP software) and measured data (ABHBC, field data and Med VI satellite image) were integrated into a GIS environment as thematic information layers and then multiplied pixel by pixel with resolutions of 30 m (international bases) and 10 m (measured data). The results of the soil loss estimation at the sites of the five abandoned quarries in the commune of Bouguergouh in Morocco showed that three quarries were located in areas with a low soil-loss rate, and two quarries were located in areas with an average erosion rate. These results were obtained from measured and international

Table 7 Soil loss for abandoned quarry sites for measured and international databases with 10 m resolution

Quarries	Soil-loss rate [10 m) (with measured databases) (t/ha/yr)	Soil-loss rate (10 m) (with international databases) (t/ha/yr)
Q1: Bouguergouh	6.33	6.45
Q2: Bouguergouh	7.7	7.82
Q3: Bouguergouh	2.83	2.95
Q4: Bouguergouh	4.16	4.26
Q5: Bouguergouh	1.28	1.36

data by setting the LS factor and using a 10 m resolution. This means the DEM 10 m is more accurate than the other DEMs and yields the same soil-loss rates. This allowed us to conclude that measured data on erosion estimation that require heavy and important resources, financial, logistical, and human (in terms of soil sampling and analysis, acquisition of high-quality/resolution data such as satellite images or climate data) can be predicted from international databases with very high resolution. However, further comparisons under different conditions are necessary to draw more general conclusions.

Acknowledgements The authors wish to express their gratitude to Hassan First University (Settat, Morocco) for financial support. We also appreciate the Royal Moroccan Center for Remote Sensing for granting our university access to Mohammed-VI satellite data at educational rates and the Bouregreg and Chaouia Hydraulic Basin Agency for supplying the precipitation data utilized in this study. We thank three anonymous reviewers for their constructive criticism, which helped improve our final text.

Author contributions The authors made equal contributions to this paper. All authors have thoroughly reviewed and approved the final version of the manuscript.

Data availability Data will be made available on request. Researchers interested in accessing the data can contact the corresponding author.

Declarations

Conflict of interest The authors declare that they have no known competing financial interests or personal relationships that could have influenced the work reported in this paper.

References

Abdi B, Kolo K, Shahabi H (2023) Soil erosion and degradation assessment integrating multi-parametric methods of RUSLE model, RS, and GIS in the Shaqlawa agricultural area, Kurdistan Region, Iraq. Environ Monit Assess 195(10):1–19. https://doi.org/10.1007/S10661-023-11796-4/METRICS

Allafta H, Opp C (2021) GIS-based multi-criteria analysis for flood prone areas mapping in the trans-boundary Shatt Al-Arab basin, Iraq-Iran. Geomat Nat Haz Risk 12(1):2087–2116. https://doi.org/10.1080/19475705.2021.1955755

Antoni V, Le Bissonnais Y, Thorette J, Zaidi N, Laroche B, Barthès S, Daroussin J, Arrouays D (2006) Modélisation de l'aléa érosif des sols en contexte méditerranéen à l'aide d'un Référentiel Régional Pédologique au 1/250.000 et confrontation aux enjeux locaux. In Etude et Gestion des Sols 13(3):201–222. https://hal.inrae.fr/hal-02663790

Aouichaty N, Bouslihim Y, Hilali S, Zouhri A, Koulali Y (2024) Assessing the influence of multiresolution DEMs on soil loss prediction using the RUSLE model in Central Morocco. Geol Soc India 100(3):426–433. https://doi.org/10.17491/jgsi/2024/173849

Aouichaty N, Bouslihim Y, Zouhri A, Koulali Y (2022) Estimation of water erosion in abandoned quarries sites using the combination of RUSLE model and geostatistical method. Sci Afr 16:e01153. https://doi.org/10.1016/J.SCIAF.2022.E01153

Aouichaty N, Koulali Y, Bouslihim Y, Hilali S (2021) Digital mapping and spatial analysis of quarries using GIS—a case study of Settat Province, Morocco. Ecol Eng Environ Technol 22(1):83–91. https://doi.org/10.12912/27197050/132091

Arnold JG, Moriasi DN, Gassman PW, Abbaspour KC, White MJ, Srinivasan R, Santhi C, Harmel RD, Griensven A, Liew MWV, Kannan N, Jha MK (2012) SWAT: model use, calibration, and validation. Trans ASABE 55(4):1491–1508. https://doi.org/10.13031/2013.42256

Bagwan WA, Gavali RS (2024) Does spatial resolution matter in the estimation of average annual soil loss by using RUSLE?—a study of the Urmodi River Watershed (Maharashtra), India. Environ Monit Assess 196(2):1–18. https://doi.org/10.1007/S10661-024-12341-7/METRICS

Beskow S, Mello CR, Norton LD, Curi N, Viola MR, Avanzi JC (2009) Soil erosion prediction in the Grande River Basin, Brazil using distributed modeling. CATENA 79(1):49–59

Bhattarai R, Dutta D (2006) Estimation of soil erosion and sediment yield using GIS at catchment scale. Water Resour Manag 21(10):1635–1647. https://doi.org/10.1007/S11269-006-9118-Z

Bleu P, Antipolis S (2003) Les menaces sur les sols dans les pays méditerranéens méditerranéens

Bonn F (1998) La spatialisation des modèles d'érosion des sols à l'aide de la télédétection et des SIG : possibilités, erreurs et limites. Science Et Changements Planétaires / Sécheresse 9(3):185

Borrelli P, Alewell C, Alvarez P, Anache JAA, Baartman J, Ballabio C, Bezak N, Biddoccu M, Cerdà A, Chalise D, Chen S, Chen W, De Girolamo AM, Gessesse GD, Deumlich D, Diodato N, Efthimiou N, Erpul G, Fiener P, Panagos P (2021) Soil erosion modelling: a global review and statistical analysis. Sci Total Environ 780:146494. https://doi.org/10.1016/J.SCITOTENV.2021.146494

Bou-Imajjane L, Belfoul MA (2020) Soil loss assessment in Western High Atlas of Morocco: Beni Mohand Watershed Study Case. Appl Environ Soil Sci. https://doi.org/10.1155/2020/6384176

Bou-imajjane L, Belfoul MA, Elkadiri R, Stokes M (2020) Soil erosion assessment in a semi-arid environment: a case study from the Argana Corridor, Morocco. Environ Earth Sci 79(18):1–14. https://doi.org/10.1007/S12665-020-09127-8

Bou Kheir R, Cerdan O, Abdallah C (2006) Regional soil erosion risk mapping in Lebanon. Geomorphology 82(3–4):347–359. https://doi.org/10.1016/J.GEOMORPH.2006.05.012

Bouslihim Y, Rochdi A, El Amrani PN, Liuzzo L (2019) Understanding the effects of soil data quality on SWAT model performance and hydrological processes in Tamedroust watershed (Morocco). J Afr Earth Sc 160:103616. https://doi.org/10.1016/J.JAFREARSCI.2019.103616

Brahim B, Meshram SG, Abdallah D, Larbi B, Drisss S, Khalid M, Khedher KM (2020) Mapping of soil sensitivity to water erosion by RUSLE model: case of the Inaouene watershed (Northeast Morocco). Arab J Geosci 13(21):1–15. https://doi.org/10.1007/S12517-020-06079-Y

Chafai A, Brahim N, Shimi NS (2020) Mapping of water erosion by GIS/RUSLE approach: watershed Ayda river—Tunisia study. Arab J Geosci 13(16):1–14. https://doi.org/10.1007/S12517-020-05774-0

Dargiri SA, Samsampour D (2023) Principles of soil erosion risk modeling. Soil erosion—risk modeling and management. IntechOpen. https://doi.org/10.5772/INTECHOPEN.111960

Devatha CP, Deshpande V, Renukaprasad MS (2015) Estimation of soil loss using USLE model for Kulhan Watershed, Chattisgarh—a case study. Aquat Procedia 4:1429–1436. https://doi.org/10.1016/J.AQPRO.2015.02.185

Dumas J (1965) Relation entre l'érodibilité des sols et leurs caractéristiques analytiques. Cahiers Orstom, pp 307–333

El-Harti A, Bannari A, Manyari Y, Nabil A, Lahboub Y, El-Ghmari A, Bachaoui E (2020) Capabilities of the new Moroccan satellite Mohammed-VI for planimetric and altimetric mapping. In: International geoscience and remote sensing symposium (IGARSS), pp 6105–6108. https://doi.org/10.1109/IGARSS39084.2020.9324290

El Jazouli A, Barakat A, Ghafiri A, El Moutaki S, Ettaqy A, Khellouk R (2017) Soil erosion modeled with USLE, GIS, and remote sensing: a case study of Ikkour watershed in Middle Atlas (Morocco). Geosci Lett 4(1):1–12. https://doi.org/10.1186/S40562-017-0091-6

El Jazouli A, Barakat A, Khellouk R, Rais J, Baghdadi MEl, (2019) Remote sensing and GIS techniques for prediction of land use land cover change effects on soil erosion in the high basin of the Oum Er Rbia River (Morocco). Remote Sens Appl Soc Environ 13:361–374. https://doi.org/10.1016/j.rsase.2018.12.004

Erdogan EH, Erpul G, Bayramin İ (2007) Use of USLE/GIS methodology for predicting soil loss in a semiarid agricultural watershed. Environ Monit Assess 131(1):153–161. https://doi.org/10.1007/s10661-006-9464-6

Ghosal K, Bhattacharya SD (2020) A review of RUSLE model. J Indian Soc Remote Sens 48(4):689–707. https://doi.org/10.1007/s12524-019-01097-0

Hagos YG, Andualem TG, Sebhat MY, Bedaso ZK, Teshome FT, Bayabil HK, Kebede EA, Demeke GG, Mitiku AB, Ayele WT, Alamayo DN, Demissie EA, Mengie MA (2023) Soil erosion estimation and erosion risk area prioritization using GIS-based RUSLE model and identification of conservation strategies in Jejebe watershed, Southwestern Ethiopia. Environ Monit Assess 195(12):1–22. https://doi.org/10.1007/S10661-023-12136-2/METRICS

Hoffmann A, da Silva MA, Naves Silva ML, Curi N, Klinke G, de Freitas DAF (2013) Development of topographic factor modeling for application in soil erosion models. In: Soil processes and current trends in quality assessment. InTechOpen Limited, London. https://doi.org/10.5772/54439

Kamamia AW, Vogel C, Mwangi HM, Feger K, Sang J, Julich S (2021) Using soil erosion as an indicator for integrated water resources management: a case study of Ruiru drinking water reservoir, Kenya. Environ Earth Sci 81(21):502. https://doi.org/10.1007/s12665-022-10617-0

Karamesouti M, Petropoulos GP, Papanikolaou ID, Kairis O, Kosmas K (2016) Erosion rate predictions from PESERA and RUSLE at a Mediterranean site before and after a wildfire: comparison and implications. Geoderma 261:44–58. https://doi.org/10.1016/J.GEODERMA.2015.06.025

Kashiwar SR, Kundu MC, Dongarwar UR (2022) Soil erosion estimation of Bhandara region of Maharashtra, India, by integrated use of RUSLE, remote sensing, and GIS. Nat Hazards 110(2):937–959. https://doi.org/10.1007/S11069-021-04974-5/METRICS

Keller B, Centeri C, Szabó JA, Szalai Z, Jakab G (2021) Comparison of the applicability of different soil erosion models to predict soil erodibility factor and event soil losses on loess slopes in Hungary. Water 13(24):3517. https://doi.org/10.3390/W13243517

Kinnell PIA (2016) A review of the design and operation of runoff and soil loss plots. In: Catena, vol 145, pp 257–265. Elsevier B.V., Amsterdam. https://doi.org/10.1016/j.catena.2016.06.013

Koirala P, Thakuri S, Joshi S, Chauhan R (2019) Estimation of soil erosion in Nepal using a RUSLE modeling and geospatial tool. Geosciences 9(4):147. https://doi.org/10.3390/geosciences9040147

Kolli MK, Opp C, Groll M (2021) Estimation of soil erosion and sediment yield concentration across the Kolleru Lake catchment using GIS. Environ Earth Sci 80(4):1–14. https://doi.org/10.1007/s12665-021-09443-7

Maury S, Gholkar M, Jadhav A, Rane N (2019) Geophysical evaluation of soils and soil loss estimation in a semiarid region of Maharashtra using revised universal soil loss equation (RUSLE) and GIS methods. Environ Earth Sci 78(5):144. https://doi.org/10.1007/s12665-019-8137-z

Millward AA, Mersey JE (1999) Adapting the RUSLE to model soil erosion potential in a mountainous tropical watershed. CATENA 38(2):109–129. https://doi.org/10.1016/S0341-8162(99)00067-3

Mitasova H, Hofierka J, Zlocha M, Iverson LR (1996) Modelling topographic potential for erosion and deposition using GIS. Int J Geogr Inf Syst 10(5):629–641. https://doi.org/10.1080/02693799608902101

Modeste M, Abdellatif K, Nadia M, Zhang H (2016) Cartographie Des Risques De L'erosion Hydrique Par L'equation Universelle Revisee Des Pertes En Sols, La Teledetection Et Les Sig Dans Le Bassin Versant De L'ourika (Haut Atlas, Maroc). Eur Sci J 12(32):277–277. https://doi.org/10.19044/ESJ.2016.V12N32P277

Mondal A, Khare D, Kundu S (2016) Uncertainty analysis of soil erosion modelling using different resolution of open-source DEMs. Geocarto Int 32(3):334–349. https://doi.org/10.1080/10106049.2016.1140822

Neitsch SL, Arnold JG, Kiniry JR, Williams JR (2000) Erosion soil and water assessment tool theoretical documentation texas agricultural eksperiment station

Oliveira AH, da Silva MA, Silva MLN, Curi N, Neto GK, de Freitas DAF (2013) Development of topographic factor modeling for application in soil erosion models. In: SORIANO, MCH soil processes and current trends in quality assessment, vol 4. InTech, Rijeka, pp 111–138. https://doi.org/10.5772/54439

Rango A, Arnoldus HMJ (1987) Aménagement des bassins versants. Cahiers Techniques de La FAO, vol 9

Ranieri SBL, De Jong Van Lier Q, SparovekFlanagan GDC (2002) Erosion database interface (EDI): a computer program for georeferenced application of erosion prediction models. Comput Geosci 28(5):661–668. https://doi.org/10.1016/S0098-3004(01)00091-7

Renard KG, Foster GR, Weesies GA, McCool DK, Yoder DC (1996) Predicting soil erosion by water: a guide to conservation planning with the Revised Universal Soil Loss Equation (RUSLE). Agric Handb 703:25–28

Roose E (1996) Land husbandry: components and strategy, vol 70. FAO, Rome

Sadiki A, Bouhlassa S, Auajjar J, Faleh A, Macaire JJ (2004) Utilisation d'un SIG pour l'évaluation et la cartographie des risques d'érosion par l'Equation universelle des pertes en sol dans le Rif oriental (Maroc): cas du bassin versant de l'oued Boussouab. Bulletin De L'institut Scientifique, Rabat, Section Sciences De La Terre 26:69–79

Saha SK (2003) Water and wind induced soil erosion assessment and monitoring using remote sensing and GIS. In: Satellite remote sensing and GIS applications in agricultural meteorology, pp 315–330

Salumbo AMdeO (2020) A Review of soil erosion estimation methods. Agric Sci 11(8):667–691. https://doi.org/10.4236/AS.2020.118043

Shan L, Yang X, Zhu Q (2019) Effects of DEM resolutions on LS and hillslope erosion estimation in a burnt landscape. Soil Res 57(7):797–804. https://doi.org/10.1071/SR19043

Shrimali SS, Aggarwal SP, Samra JS (2001) Prioritizing erosion-prone areas in hills using remote sensing and GIS—a case study of the Sukhna Lake catchment, Northern India. Int J Appl Earth Obs Geoinf 3(1):54–60. https://doi.org/10.1016/S0303-2434(01)85021-2

Singh RP, Huerta-Espino J, Sharma R, Joshi AK, Trethowan R (2007) High yielding spring bread wheat germplasm for global irrigated and rainfed production systems. Euphytica 157(3):351–363. https://doi.org/10.1007/s10681-006-9346-6

Tahiri M, Tabyaoui H, Tahiri A, El Hadi H, El Hammichi F, Achab M (2015) Modelling soil erosion and sedimentation in the Oued Haricha sub-basin (Tahaddart watershed, Western Rif, Morocco): risk assessment. J Geosci Environ Prot 4(1):107–119. https://doi.org/10.4236/gep.2016.41013

Taoufik M, Loukili I, Hadi HEl, Baghdad B (2020) Soil erosion risk assessment in an extraction area: case of abandoned quarries in the Akreuch region (Morocco). In: Proceedings—2020 IEEE international conference of Moroccan geomatics, MORGEO 2020, pp 1--5. https://doi.org/10.1109/Morgeo49228.2020.9121910

Thapa P (2020) Spatial estimation of soil erosion using RUSLE modeling: a case study of Dolakha district, Nepal. Environ Syst Res 9(1):1–10. https://doi.org/10.1186/S40068-020-00177-2

Wang G, Gertner G, Fang S, Anderson AB (2003) Mapping multiple variables for predicting soil loss by geostatistical methods with TM images and a slope map. Photogramm Eng Remote Sens 69(8):889–898. https://doi.org/10.14358/PERS.69.8.889

Weslati O, Serbaji MM (2024) Spatial assessment of soil erosion by water using RUSLE model, remote sensing and GIS: a case study of Mellegue Watershed, Algeria-Tunisia. Environ Monit Assess 196(1):1–26. https://doi.org/10.1007/S10661-023-12163-Z/METRICS

Williams JR, Singh V (1995) The EPIC model. Computer models of watershed hydrology. Water Resourc Publ Highl Ranch Colorado 25:909–1000

Wischmeier WH, Smith DD (1978) Predicting rainfall erosion losses: a guide to conservation planning (Issue 537). Department of Agriculture, Science and Education Administration

Zhang Y, Zhang M, Niu J, Li H, Xiao R, Zheng H, Bech J (2016) Rock fragments and soil hydrological processes: significance and progress. CATENA 147:153–166. https://doi.org/10.1016/j.catena.2016.07.012